Per LINDH [1,2], Polina LEMENKOVA [3]

Permeability, compressive strength and Proctor parameters of silts stabilised by Portland cement and ground granulated blast furnace slag (GGBFS)

The study investigates the effect of Portland cement and ground granulated blast furnace slag (GGBFS) added in changed proportions as stabilising agents on soil parameters: uniaxial compressive strength (UCS), Proctor compactness and permeability. The material included dredged clayey silts collected from the coasts of Timrå, Östrand. Soil samples were treated by different ratio of the stabilising agents and water and tested for properties. Study aimed at estimating variations of permeability, UCS and compaction of soil by changed ratio of binders. Permeability tests were performed on soil with varied stabilising agents in ratio $H_W L_B$ (high water / low binder) with ratio 70/30%, 50/50%, and 30/70%. The highest level of permeability was achieved by ratio 70/30% of cement/slag, while the lowest – by 30/70%. Proctor compaction was assessed on a mixture of ash and green liquor sludge, to determine optimal moisture content for the most dense soil. The maximal dry density at 1.12 g/cm^3 was obtained by 38.75 % of water in a binder. Shear strength and P-wave velocity were measured using ISO/TS17892-7 and visualised as a function of UCS. The results showed varying permeability and UCS of soil stabilised by changed ratio of CEM II/GGBS.

✉ Per Lindh, email: per.lindh@byggtek.lth.se

[1] Swedish Transport Administration, Malmö, Sweden. ORCID: 0000-0002-0577-9936

[2] Lund University (Lunds Tekniska Högskola LTH), Faculty of Engineering, Department of Building and Environmental Technology, Division of Building Materials, Lund, Sweden.

[3] Université Libre de Bruxelles (ULB), École polytechnique de Bruxelles (Brussels Faculty of Engineering), Laboratory of Image Synthesis and Analysis, Brussels, Belgium. ORCID: 0000-0002-5759-1089, email: polina.lemenkova@ulb.be

1. Introduction

1.1. Background

The fundamental structure of soil includes important morphometric parameters, such as size, shape and aggregation of granules, size and density of pores and arrangement of elements within the soil mass. In turn, these largely influence its physical and mechanical properties, as reported in previous studies: strength [1], compactness [2–4], penetration resistance, permeability [5, 6], air-filled porosity [7–9] and gas diffusivity [10]. Besides, the cohesion [11, 12] and friction angle of soil [13–15] are important parameters that affect slope stability through anisotropy of the shear strength [16, 17] and have a notable effect on the effective stress and the dynamic pore pressure in soil [18]. Thus, these soil parameters are crucial for construction industry when evaluating stability and deformation of geotechnical structures, as soil strength affects stability, durability and safety of structures [4, 19–22].

The performance of soil properties over time with changing external loads, treatment chemical agents or varying environmental conditions, such as temperature or humidity, can be evaluated through a series of practical experiments. These include, among others, measurement of strength, porosity, compactness and permeability that can be evaluated using various geotechnical devices and existing practical workflow manuals [23, 24]. For instance, because soil is a complex structure consisting of solid particles and voids filled with water and/or air, its compactness and porosity can be assessed by evaluating water content and dry density [25]. The correlations between hydraulic, physical and mechanical properties of soil can be found by quantifying water content in its pore structure, which is possible by measuring soil permeability [26]. Practical engineering testing of soil is a key procedure for evaluating its bearing capacity in order to ensure safety of the infrastructure and avoid possible damages [27–30].

Evaluating soil parameters has a goal of assessment its strength prior to the earthworks, because safety of infrastructure is largely influenced by soil compressibility as much as by compressive strength. Therefore, physical and mechanical properties of soil should be tested and improved in order to increase strength and bearing capacity. This is often a case for weak compressible soils, such as silt and clays. The improvement of properties and behaviour of weak soil is performed through the stabilization and solidification (S/S). The procedure of soil stabilisation is developed and evaluated in many reports on civil engineering [31–34]. They described the improvement of compression characteristics of soil, required prior to construction or civil objects. The stabilisation improves stiffness and durability of the soil-binder system because the initial natural voids and pores of the raw soil structure become filled by binders that increase the soil strength. As damages or cracks in weak soil may affect lives, the importance of soil testing is clear.

The process of soil stabilisation consists in adding stabilising agents, or binders, into the soil mass. The impact of admixtures on soil strength depends on a variety of factors, among which soil type is one of the primary ones. Curing conditions are key factors in soil stabilisation which aims at increasing its strength through mixing up soil with binding agents [35–37]. Temperature and time are the most important curing parameters which have a strong effect on soil strength development [38–40]. In general, the unconfined compressive strength of the stabilised soil increases along with curing time, as noted earlier in previous works [32, 41, 42]. Other parameters include curing stress, confining pressure, content and combination of cement/admixture, proportions of water/binder ratio, soil types, porosity and organic matter content [43–46]. Besides, changing rate of continued hydration process and elevated moisture results in binding of cementitious products between the adjacent soil particles in the course of curing which increases to soil strength. For example, strength and modulus of soil increase along with curing time and temperature, as well as ratio of cement in a binder mixture [47].

The type and amount of binder strongly affect the strength of the stabilized soil. The most common stabilising agents are cement [48], cementitious products, such as fly ash [49, 50], cement kiln dust [51, 52], and lime [53–56]. The by-products of the industrial processes or iron and steel-making, such as ground granulated blast furnace slag (GGBFS) [57] and sludge [58, 59] can also be used as binders. Besides the type of binders, the process of soil stabilization includes practical estimation and determining the amount and ratio proportions of admixtures in tested soil samples, which also affects its compressive strength and microstructure [60, 61].

Soil compactness, permeability and compressive strength are important technical properties measured during the S/S procedure prior to construction works [62, 63]. Extensive literature is available on the S/S of soil and measuring its properties including soil types, testing methods and reported results [64–67]. Fewer studies focused on soil compaction and the impact of binder ratio on stabilization, permeability and compressibility [68, 69]. Soil compaction is resorted in a weak clay aimed at improving its compactness and density by reducing void space, *i.e.*, the amount of air between the granules. Hence, the evaluation of soil compactness is related to the measurement of shape indices of pores and solid phase elements [70]. The importance of compaction of clayey soil consists in its applicability as a frequently used material in construction industry due to physical and mechanical properties of compacted clays [71].

The Proctor compaction test is a commonly used technique for measuring soil compactness aimed at assessing safety and bearing capacity of roads, pavements and building foundations. It has advantages in the approach and robustness of the workflow [72–74]. Its applications include geotechnical engineering [75, 76] and agriculture [77–80]. Besides Proctor test, existing methods are developed to standardise the procedure of compaction tests [81, 82]. These are used to determine the relationship between the moulding water content and dry unit weight of soils. Other examples of testing soil compactness include gyratory compactor [69],

vibrating compaction, modified Proctor compaction on the stress-strain characteristics and shear strength [83] or using oedometer for testing texture and macropores after compression of the compacted soil [84]. The Soil Classification System developed by the American Association of State Highway and Transportation Officials (AASHTO) is used for soil quality assessment in highway construction industry. For example, it is tested for measuring density and moisture content of soil [85].

Since soil has a permeable structure due to the voids in pores, testing soil permeability is required for a variety of geotechnical works, e.g., analysis of seepage, dewatering, evaluating possible water flow through soil. The tests on soil specimens are used to measure soil permeability, using laboratory approaches [86] or in the field using borehole tests [87], by *in-situ* field measurements [88], e.g., using piezocone penetration and dissipation tests [89, 90]. A more straightforward and theoretical approach is a numerical modelling of the pore structures of soil aimed at computing the coefficient of permeability based on the laboratory evaluations of soil samples, such as the grain size distribution [91].

The compressive strength of stabilised soil is measured by the unconfined compression test, a standard approach widely used in various geotechnical engineering applications [92, 93]. The advantages of this method include the reliability and robustness of the approach, fast workflow process and affordable measurement equipment. Testing compressive strength is applicable to saturated, cohesive, fine-grained soil samples [94, 95]. The idea behind the compressive strength testing is to control strain of soil samples through changes in pores of the soil sample under pressure. This method enables one to obtain an estimate of the soil strength and to determine its applicability for effective and safe construction. The compressibility and strength of soil are a basic frame for the interpretation of the characteristics and suitability of soil. The physical and mechanical properties of soil depend on its inherent natural structure, *i.e.*, fabric and bonding characteristics [96]. Binders react with water and show a bonding effect that contributes to the increase of the compressive strength of soil. Soil stabilisation results in its higher strength.

1.2. Study objectives

The present study examines physical and mechanical properties of soil: compression strength, permeability and compactness. The study goal is to evaluate the compressive strength, permeability and compaction of the stabilised soil prepared for the construction works. The specific objectives of this study include the following tasks:

1) to analyse grain size distribution;
2) to determine values of the UCS for each mixture of soil samples stabilised by various binder/water ratio (low/high) and stabilising agents (cement/slag): 70/30%, 50/50%, 30/70%;

3) to assess soil permeability through a series of the duplicate tests performed for different soil/binder proportions ($H_W L_B$, $L_W H_B$, $L_W E L_B$) with cement/slag for high-low soil and binder ratios;

4) to perform Proctor compaction test and visualise soil curves to evaluate the degree of maximum moisture content at which soil is the most dense and achieves maximum dry density;

5) to find a correlation between the ultrasonic P-waves velocities and the UCS of soil with various amount of binder (120 and 150 kg/m^3);

6) to observe the variability in values of the P-wave velocity for soil taken from sample sites A4 and B4 and stabilised by various amount of binder, and to statistically visualise the difference on the histograms;

7) to compare changes in the P-wave velocity with values of the UCS for all samples from various phases of the experiment and binder ratios and to visualise them on a graph.

Existing works in civil engineering and geotechnical testing of soil mostly focus on the effectiveness of various types of binder as a stabilising agent, e.g., lime [97–99], and fly ash [100]. Others reported testing soil types: such as frozen soils [101, 102], sand soil [103], clay or silt [104]. Some works discuss technical issues of data processing [102, 105]. In this study we evaluated the effects of varying ratio of binders assessed as a two-factor experiment. We analysed the ratio of the binder/water content in a soil mass to find the optimal admixture proportions to increase soil strength. Finally, we tested the effects of adding the green liquor sludge and ash on soil compaction. We used two binders: Portland cement and slag. In the experiment, we used the three technical workflow phases: Phase 1, 2 and 3, where Phases 1 and 2 are the fieldwork-based experiments, while Phase 3 is a scaled-up experiment. We used three levels of binder quantity in kg/m^3 of soil that differed in each phase: 150 kg and 120 kg in Phase 1, 100 in Phase 2 and 150 kg in Phase 3.

2. Methodology

This section describes the type, properties and the origin of the soil material used in this study, as well as methods used to perform experiments. The evaluation of the soil properties was based on considering various criteria which include regional soil type, amount and ratio of binders used for treatment of dredged samples, and the ISO standard requirements for workflow used from the existing standards. Soil samples were treated by different ratio of the stabilising agents and water and tested for physical and mechanical properties. Evaluating soil properties aimed at assessing its bearing capacity for planned engineering construction works.

A series of the tests was performed on the three soil mixes treated by varied binder ratios of cement/slag, aimed at determining soil compaction by Proctor characteristics, UCS and permeability. The methodology included the factorial experiment which was used for each admixture to evaluate the effects of the changed

water ratio and the amount of binder as variables. The velocities of the ultrasonic P-waves were measured using existing methods [32] to determine soil strength. The techniques were adopted from the standard guidance determining the workflow for testing soil. This included devices, curing time, workflow, type and amount of binder used as stabilising agents for soil. The methodology included a series of experiments performed in the laboratory of the SGI, Gothenburg, including processing, curing, testing and stabilization. The workflow followed the guidance documented by the Swedish Institute for Standards (SIS) [106–108].

The samples firstly were compacted and evaluated by Proctor test and then tested for permeability. Testing soil permeability aimed at estimating possible danger of soil swelling caused by the effective stress in a non-stabilised soil. For example, swelling of roads is caused by permeability of soil and excess of water which depends on the environmental and climate setting. The soil permeability was measured in the laboratory using SIS methodology [108]. The workflow included a series of tests made using pressure permeate method (SGI standard, edition 15).

2.1. Materials

Soil samples were dredged from the site prepared for construction works on behalf of the SCA Biorefinery Östrand AB. The specimens were collected in a test site located in the coastal area of Timrå municipality, Östrand area of the Bothnian Bay, Baltic Sea, Sweden, Fig. 1. The sampling has been performed on various sites, Nr. A1–A8, B1–B24, Fig. 1.

Fig. 1. Study area: coastal area of Timrå municipality, Bothnian Bay, Baltic Sea. Numbers (A1–A8, B1–B24) indicate position for taking sites where sediment samples were collected and groundwater samples taken. Figure source: SCA Biorefinery Östrand AB

The sieve analysis was used to determine grain size distribution. The soil types of the samples are presented by the boreal clays and loamy silts followed by sand and gravel. The grain distribution analysis was performed on the aggregated dredged samples to determine the ratio (%) of size of soil grains in the soil samples and to predict soil behaviour based on the morphology and size of the soil granules. The curvature of the soil grain distribution reflecting particle size analysis was used to classify soil types. The results of test are shown in Fig. 2 which visualises grain size distribution curve for a selected specimen using random soil sample. The sample volume was 3.212 g.
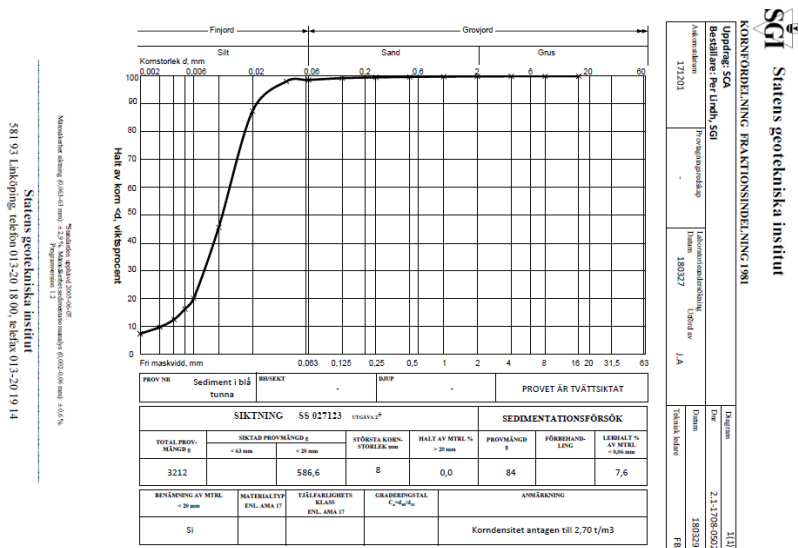
Fig. 2. The grain distribution diagram for aggregated sample collected from the site B6b. The laboratory tests of soil sieve analysis and curve plotting were performed at the SGI by Per Lindh

The results of the sieve analysis show that the dominating type of samples was fine-grained silt, followed by a fraction of coarse sand and gravel, Fig. 2. The sifted test amount included 586.6 g of the material samples with size of < 20.0 mm, that is, a fine-grained silt. The largest grain size was detected as 8 mm of size, Fig. 2. The basic mineral formatting element in a tested material is Silicon (Si). The grain density was 2.70 t/m^3. The clay content in percentage of the tested soil material < 0.06 mm was 7.6%. A large proportion of fibre was also presented in the samples, Fig. 3.

Two types of binders were used as stabilising agents: Portland cement (type Basement CEM II / A-V, SS EN 197-1) and ground granulated blast furnace slag (GGBFS). The cement is of composite type with mixtures of Portland cement, slag and Pozzolana. It is a Portland-fly ash cement with proportions of mixture of clinker between 80–94%, siliceous fly ash in between 6–20%, and minor additional

constituents between 0–5%. The slag Bremen, or GGBFS, is a mineral additive material (type II) with latent hydraulic properties, used as a binder according to the standard SS 137003 [109].

Fig. 3. Photo showing dried material after washing sieving. Note the amount
of fibre at the top of the image. Photo by Per Lindh

The slag Bremen comes from iron production in Germany from where it derived its name, and is a quality-assured and CE-marked additive material that meets the requirements of SS EN 151671 and 151672 standards. The slag Bremen has a compact density of 2900 kg/m^3, which can be compared with cement which has a density of about 3100 kg/m^3, and a bulk density is ca. 1150 kg/m^3 (cement is ca. 1250 kg/m^3) [110].

2.2. Sampling process

The sampling method has taken as the input a set of the bottom sediments which were collected using the bucket with size of about 1 m^3. The main steps of sampling are as follows: soil was dredged in the sampling points by one scoop per point. We placed soil sediments from each test point into the separate containers, in order to localise the samples. The representative sediments were kept below the water level to maintain natural conditions of the marine sediments. We extracted a set of soil samples from each soil container and sent to the SGI for further processing and tests which included measuring compaction, performing Proctor test, evaluating compressive strength ratio, permeability and sieve analysis of soil. The soil sample were homogenised in each corresponding container by mixer during five minutes to achieve the representative samples. Afterwards, binder mixed with soil samples in different proportions and water ratio. The stabilized soil samples were then filled into plastic containers by filling fifteen sampling sleeves. The specimens were stabilized in varied recipes and kept in the containers with closed lids.

2.3. Phase 1

The stabilisation of soil adopted existing general procedure requirements developed by CEN [107]. To optimise the workflow, a special methodology was used based on the statistical experimental planning. The experimental trials of the soil mixture were used to find the optimal ratio of water and binder. We used Portland cement and GGBFS as stabilising agents of soil in mixes in three varied proportions in the following ratios: 70/30%, 50/50%, and 30/70% of cement and slag.

The mixes contained silt, followed by insignificant amount of sand and gravel. Following the pre-processing and curing of samples, we tested strength (UCS), compactness (Proctor modified compaction test) and permeability of soil. Three different binder combinations and ratio between binder and water content were evaluated, Fig. 4. In addition, the effect of varied water ratio was tested with different quantities of the stabilising agents (cement and slag) in Phase 1.
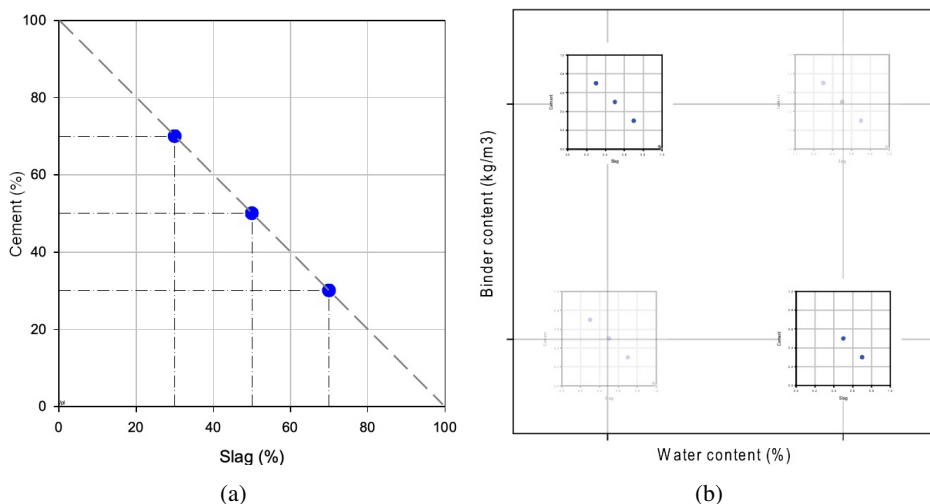
Fig. 4. (a) Binder combinations of Portland cement and slag (GGBFS); (b) Factorial experiment with water ratio and amount of binder as variables

The samples included mixes of cement and slag with appropriate proportions at 120 and 150 kg of binder volume per m^3 of the dredged silt. The workflow included simultaneous evaluation of soil mixes that consisted of the dredged masses of silt. Tested samples consisted of various binder proportions and water ratio which provided information on soil properties that can be used to control the *in-situ* earthwork process in the field. A graph in Fig. 4a shows the three tested binder combinations of Portland cement and slag (GGBFS). The cement tested was Bascement and the slag was Bremen slag. The graph in Fig. 4b shows a factorial experiment with water ratio and amount of binder as variables.

High and low water ratios in these tests consisted of 190 or 139% (that is, excess of water), while high and low amount of binder consisted of 150 and 120 kg/m^3 of binder per m^3 of the silt mass, respectively. The combination of the high water ratio (H_W) and low amount of binder (L_B) constitutes a "worst case scenario" as the material risks having a higher permeability and lower technical strength. The scenario will be referred to as "high water – low binder" ($H_W L_B$). The opposite case, "low water content – high amount of binder", gives 'the best case', i.e., a material with low permeability and high technical strength. This combination is further referred to as ($L_W H_B$). Fig. 5 shows the best and worst ratios marked in a matrix based on factor experiments, i.e., two variables tested at two levels mentioned as "high" and "low").
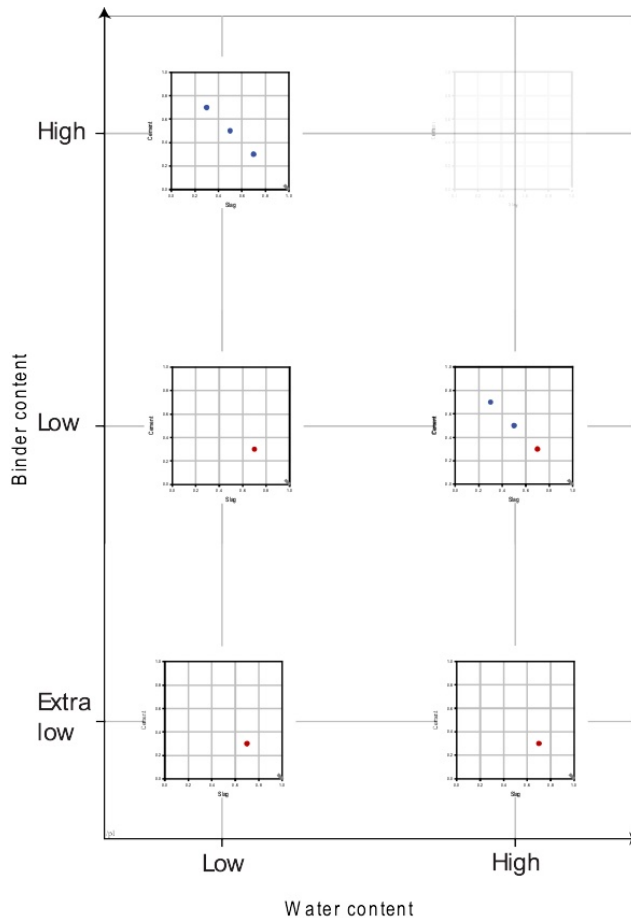
Fig. 5. Graph showing the setup of Phase 1 and 2 of the experiment. Here Phase 1 is indicated by the blue dots, Phase 2 – by the red dots. Blue circles show where Phases 1 and 2 overlap. High and low water ratios in these experiments consisted of 190%, respectively 139% (that is, excess of water). High, low and extra low amount of binder consisted of 150, 120 and 100 kg/m^3

2.4. Phase 2

Upon the trial testing and evaluation of soil mixtures in Phase 1, suitable recipes were selected in Phase 2. The additional amount of binder was added to soil samples in Phase 2: 100 kg of binder per m^3 of soil. Compared with the experimental setup in Phase 1, the minimum amount of binder was reduced to 100 kg/m^3. The reduction was based on the existing technical requirements on strength and permeability of the stabilised soil. The goal of the Phase 2 was to optimise the cost of the recipe without losing technical / environmental quality of soil. The optimisation of the recipe also contributed to the decline in CO_2 emissions during the industrial works. The performed test combinations are presented in Fig. 5 which shows the experimental setups of Phase 1 and 2. Here the Phase 1 is indicated by the blue dots and the Phase 2 – by the red dots, respectively. High and low water ratio in tests consisted of 190% and 139% (excess). High, low and extra low amount of binder consisted of 150 kg and 120 kg for 100 kg/m^3. Compared to the Phase 1, the minimum amount of binder was reduced to 100 kg/m^3 of the dredged material.

2.5. Phase 3

The Phase 3 refers to the scaled-up experiment. This part of the experiment included adding 150 kg of binder to the tested soil mass. Notable results from the Phase 3 include the highest values of the velocities of P-waves which indicated high strength. This is caused by the maximal amount of binder used in this part of the experiment, which contributed to the overall increase of strength of soil.

3. Results and Discussion

3.1. Proctor compaction test

The Proctor compaction test was performed on soil samples using an addition of mixture of ash and green liquor sludge from the SCA's plant. The aim was to determine the optimal moisture content at which soil becomes the most dense and reaches a maximal dry density. The Proctor test was applied in a modified approach which enables us to evaluate the compaction of soil after stabilisation and changed content of structure within the soil mass. The mutual ratio was 50/50% calculated on the dry material. The Proctor tests were performed according to the Swedish standard SS027109 (Laboratoriepackning (Proctor) per packat prov, SS027109). The optimal water ratio was recorded as about 39% at which level it was possible to achieve the best compaction of soil, *i.e.*, the highest dry density (Fig. 6). The maximal dry density at 1.12 g/cm^3 was achieved by 38.75% of water in a binder. The obtained data were statistically processed and tested using the Least Square method, Singular Value Decomposition (SVD) algorithm.
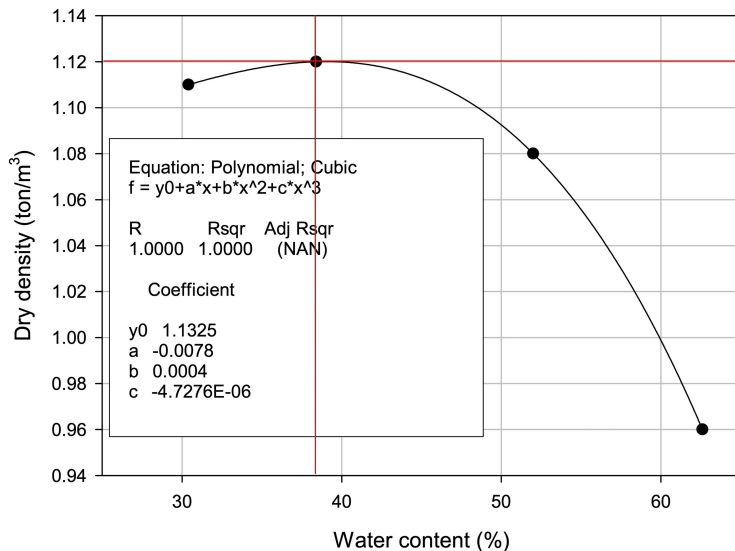
Fig. 6. Results of the Proctor compaction tests of green liquor sludge and ash. $W_{opt} \sim 39\%$.

The results of the test are presented in Fig. 6 (Proctor compaction test) showing correlation of soil compaction through the dry density of soil and water content in a binder. Thus, there is a correlation between the soil composition, the degree of carbonation of the ash and the water ratio of the green liquor sludge. Changes in the maximal dry density depending on water content in a binder indicated that wetness of soil processed by the green liquor sludge and ash could be used to predict variation of soil compactness with changed ratio of water in the diapasons between 30%–65% (Fig. 6). The maximal peak of the dry density of soil was achieved by water content of 38–39% in the soil mass. After that, the soil dry density decreased exponentially along with the increase of water content in the soil sample until 65% (*i.e.*, a maximally measured value). The results of the Proctor tests demonstrated that dry density is sensitive to the changes in soil wetness.

3.2. Soil permeability

The evaluation of permeability included the calculation of the permeability coefficient in treated samples, compared for each case of various ratios of binder and water, Table 1. In general, within each group of tested soil samples, the permeability decreases along with the increasing amount of added cement, Fig. 7. This is explained through the bonding of the soil particles together and water proofing by the binding agents. Thus, adding binders to soil improves its strength and increases resistance to softening by water. The test has been performed using a double sampling method where data distribution within each group demonstrates a decrease along with the increasing amount of binder: cement and slag.
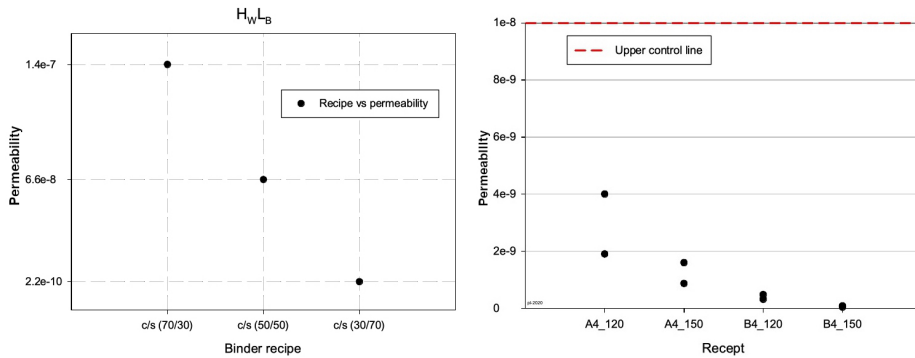
(a) Permeability of $H_W L_B$ with cement/slag ratio: 70/30%, 50/50%, 30/70%

(b) Permeability duplicate tests for the different soil and binder ratios (all samples)

Fig. 7. Permeability tests on the stabilised soil with varied stabilising agents in different binder ratios

The specimens tested for permeability in Phase 1 were considered for the worst-case scenario, *i.e.*, only samples from the $H_W L_B$ series ratio, *i.e.*, 'high water / low binder'. Despite this, the results showed 'low to very low' degrees of permeability, see Fig. 8. As a result of testing, samples with an increased slag content gave a denser material. The eight permeability tests were performed in total in the laboratory during the Phase 2 of the experiment. The optimal recipe consisted of 30% cement and 70% slag at the two different amounts of binder and water quotas, which made it possible to achieve the quality requirement of 10^{-8} m/s, that is, low water and low binder ratio (sample 1, $L_W L_B$), high water and high binder ratio (sample 4, $H_W H_B$) and low/high water and high binder ratio (samples 6 and 8: $L_W H_B$ and $H_W H_B$), respectively. The results are shown in Table 1.
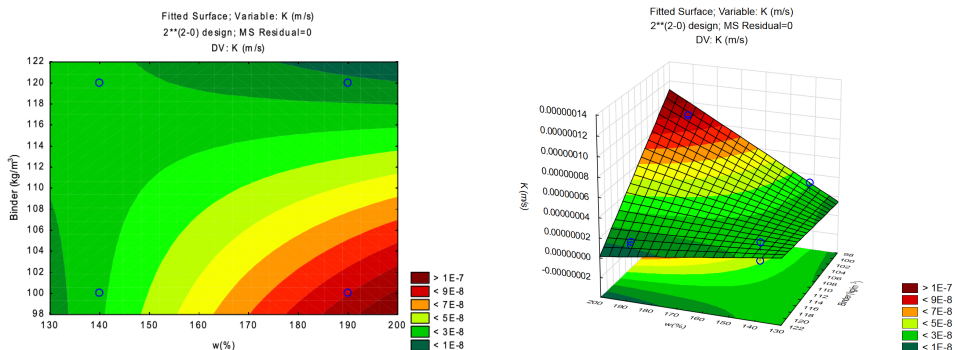
(a) Permeability of $H_W L_B$ with cement/slag ratio 70/30%, 50/50%, and 30/70%

(b) Permeability duplicate tests for the different soil and binder ratios (all samples)

Fig. 8. Permeability tests on the stabilised soil with varied stabilising agents in different binder ratios

Table 1. Coefficient of permeability K tested in SGI laboratory during Phase 2 of the experiment

No.	Water ratio (%)	Binder (kg/m^3)	Permeability, K (m/s)
1	140	100	$1.9\,E^{-8}$
2	140	120	$3.2\,E^{-8}$
3	190	100	$8.7\,E^{-8}$
4	190	120	$1.4\,E^{-8}$
5	140	100	$3.7\,E^{-8}$
6	140	120	$1.4\,E^{-8}$
7	190	100	$9.2\,E^{-8}$
8	190	120	$1.1\,E^{-8}$

The response area from the analysis is reported in Fig. 7 (permeability of $H_W L_B$ with changed cement/slag ratios and permeability duplicate tests for all samples). In the yellow-red areas, a significant interaction is shown between the change in the amount of binder and water ratio. The correlation results in a sharp deterioration in soil quality through the increased permeability from 10^{-7} m/s to 10^{-8} m/s. Strong interaction demonstrates the importance of working with finely adjusted recipe optimisation at the laboratory level during soil testing.

Changing binder ratios enabled a better control of the mixing process in the *in-situ* field sampling, so that quality requirements were achieved and project uncertainties were reduced. A robust recipe of the soil mixture with binders included 120 kg of binder per m^3 of the dredged silt aimed at providing a sufficiently low permeability level at several different water quotas during the tests. A graph showing the permeability of the $H_W L_B$ with changed ratio of binders Portland cement/slag is shown in Fig. 7a. The results of the permeability tests show different materials and binder ratios. The duplicate experiments have been performed on all the samples. The permeability gradually decreased along with added slag and reduced Portland cement, and vice versa, within each case of mixture, Fig. 7b.

Fig. 8a shows a 2D response area for the permeability tests. The results show a strong negative interaction between the binder content and water ratio. Fig. 8b shows a 3D response area for the permeability tests. The results show a strong negative interaction between binder content and water ratio. Thus, at higher water ratio and lower amount of binder, the permeability increases in 10 times for both cases, Fig. 8a and 8b. All tests are performed as double tests during Phase 2.

3.3. Compressive strength

The use of the ultrasonic P-waves in geotechnical tests is a modern non-destructive method aimed at analysing the strength of the stabilised soils. The applicability of this method consists in the relationship between the velocity of P-wave propagation and mechanical, structural and elastic properties of soil that largely control the velocity of P-waves. Solving the inverse problem, the measured P-wave velocity can indicate the soil strength. Besides that, evaluating P-wave

velocity provide a rapid, robust and reliable approach as an alternative to the existing traditional methods of testing soil strength. For example, it can be used for detecting early micro damages in building materials [111]. Therefore, we estimated P-wave velocities to evaluate strength of the stabilised soil.

The soil specimens had a diameter of ca. 50 mm and a height of ca. 100 mm. The compressive strength of soil was determined according to the ISO/TS 17892-7 standard using technical guidance of SIS [106]. The deformation rate was about 1% / min which gives an approximate speed of 1 mm/min of wave propagation through a specimen. The results of the UCS tests are shown in Fig. 9. The shear strength and the P-wave velocity of soil were measured using the CEN 16907-4 standard and visualised as a function of the UCS. The shear strength of the tested samples was obtained by multiplying the UCS values by 0.5. All the recipes meet the requirements for a minimum compressive strength of 280 kPa, compared with the laboratory tests. The UCS and P-wave velocities were recorded for the samples taken from the sites A4 and B4 with 120 and 150 kg of binder per m^3 of soil. The graphs have been visualised as statistical plots for each mixture in 4 cases (Figs 9 and 10).
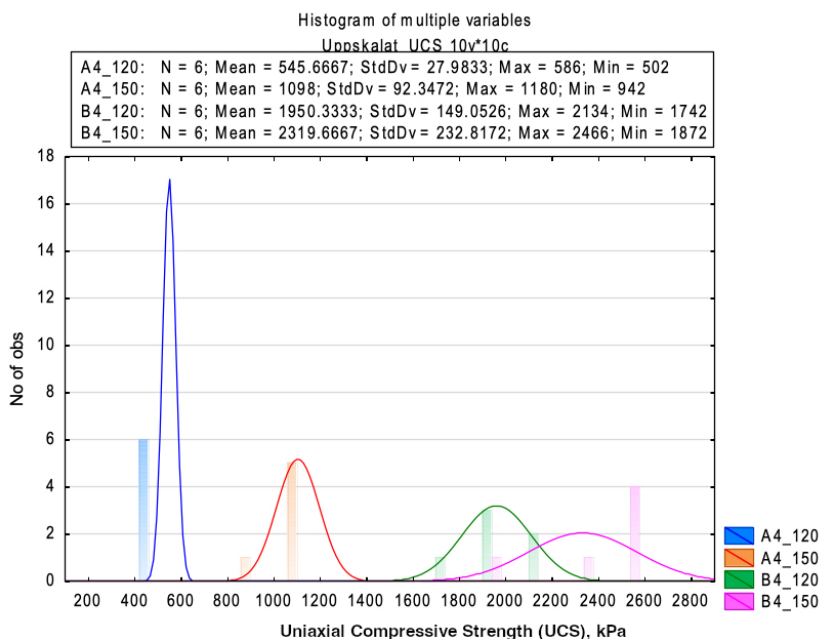
Fig. 9. Uniaxial Compressive Strength (UCS) tests for each mixture

The results of the UCS tests for each mixture are shown in Fig. 9. For material taken from the A4 site (see map with location of test sites in Fig. 1) with a water ratio of about 135%, an increase in the amount of binder means a doubling in strength. This effect is not visible for the soil material taken from the B4 site (Fig. 1) where
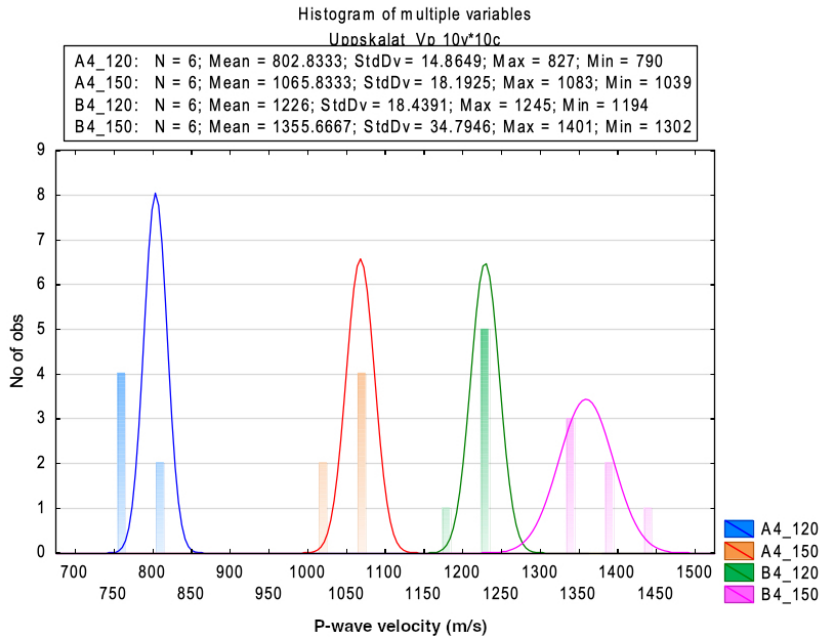
Fig. 10. Histogram showing P-wave velocity for materials taken from the A4 and B4 sample sites with 120 and 150 kg of binder per m^3 of the dredged material

the water ratio was about 69%. Different amounts of binder are shown in the legend of Fig. 9: 120 and 150 kg for each case, respectively. The variation in the P-wave velocity with changed compression characteristics of the stabilized soils was also evaluated.

Fig. 10 shows the histograms for the P-wave velocity of soil specimens collected in sites A4 and B4. Similar to the results of the UCS tests, this graph shows the empirical data distribution for each case. Scattering increases along with the increasing P-wave velocity. However, the increase in data distribution is in general lower and the overlap between the B4_120 and B4_150 is considerably lower. The B4_120 shows the graph for soil collected from the test site B4 stabilised by 120 kg of binder, while B4_150 is the same, stabilised by 150 kg of binder.

The P-wave velocity has been measured for each case of binder combinations ($H_W L_B, L_W H_B, H_W E L_B, L_W E L_B$), that is, the abbreviations stand for "High Water / Low Binder, Low Water / High Binder, High Water / Extra Low Binder, Low Water / Extra Low Binder" (Fig. 11). The highest values of the P-waves were recorded in the case of Phase 3, where the experiment included 150 kg of binder as an admixture to the soil (red stars in the graph). The lowest values were recorded for the Phase 2 of the experiment, where 100 kg of binders were added. In Phase 1, two levels of binder quantity per m^3 of the dredged material were tested: 150 kg and 120 kg: red squares in Fig. 11.
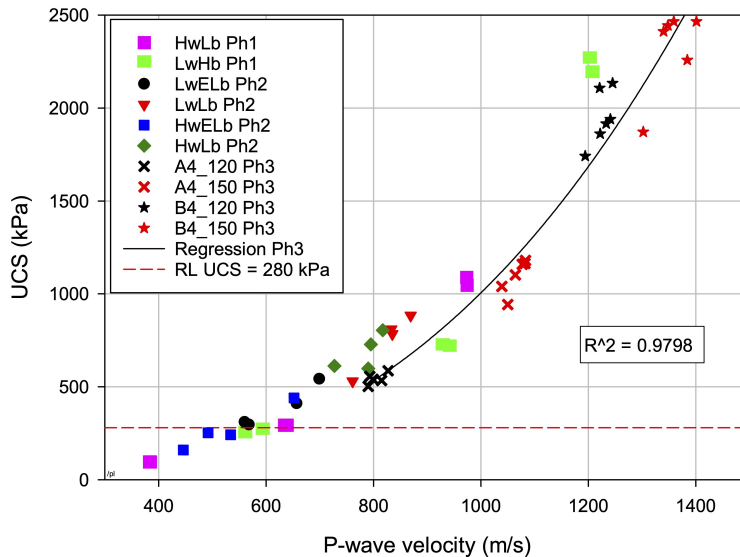
Fig. 11. The correlation between P-wave velocity and compressive strength of soil for all samples tested at various phases of the experiment and using different binder ratios

Fig. 11 shows the results of the measured P-wave velocity in soil as a function of the compressive strength and the admixture of binders in various ratios. The compressive strength shows a complex characteristics of the soil largely influenced by the soil structure. This includes a variety of parameters, such as voids, pores, imperfections, specific local defects in a given specimen. Therefore, a relationship between the compressive strength and the velocity of P-waves is shown as a curve rather than a direct straight line. Nevertheless, a higher P-wave velocity is in general associated with a higher compressive strength of soil, Fig. 11.

As mentioned above, the velocity of P-waves passing through the soil sample generally increases with the increasing compressive strength of this soil specimen. However, a certain difference between the laboratory results and the scaled-up experiments can be seen for each recipe of binder ratios tested during different phases of the experiment. Thus, the Phase 1 was the initial stage of the laboratory experiments, while the Phase 2 is a supplement with a lower binder content, which included the optimisation phase aimed at finding a lower limit for the amount of binder. The Phase 3 refers to the scaled-up experiment in this study.

The results show similar patterns of strength for different phases with various amount of binder added into the soil masses. The difference in variation is also supported by the results received from other previous projects, e.g., Arendal 2, Gothenburg and Kolkajen, Stockholm. A certain displacement can be discerned by comparing these data, i.e., slightly lower strength at the same P-wave velocity for the scaled-up experiment in Phase 3. The results are in general consistent with the expected variation based on the comparable similar geotechnical surveys of soil.

The compressive strength of soil correlates with the stiffness of the specimens collected from the testing sites A4 and B4 during Phases 1, 2 and 3 of the experiment. It is reflected in variations of the velocity of the P-wave propagation in various binder ratios ($H_W L_B$, $L_W H_B$, $H_W E L_B$, $L_W E L_B$). The relationship between the P-wave velocity and the compressive strength of soil changed in various combinations of binders (Portland cement/GGBFS) and water for each mixture, as shown in Fig. 11. The trends observed in the comparison of "P-wave velocity-compressive strength" graphs are pronounced and show the direct correlation between the parameters of P-wave propagation and soil stiffness.

4. Conclusions

This study presents the evaluation of soil strength, compactness and permeability with a case of stabilised loamy silts. We used methods of UCS, permeability tests and modified Proctor test. Soil density was assessed using the modified Proctor compaction tests by heavy laboratory compaction. The Proctor method was effective in evaluating the compactness of soil and demonstrated a tight correlation between water ratio in the pores and dry density of soil.

Soil strength was estimated using applied geophysical methods. We evaluated the velocity of P-waves passing through the soil samples stabilised by various proportions of cement/slag for comparison of their effects. The amounts of binder/water were also changed to find the optimal ratio with the best effect on stabilisation. Using the experimental changes of binders we have demonstrated their effects on soil strength. Estimating P-wave velocities proved to be a fast, robust and reliable method for evaluating soil strength. Its advantages include repeatability of testing, reduced number of tests and optimised workflow.

We demonstrated that the stabilisation of soil by various amount of binder improves its parameters: increased compressive strength, compactness and decreased permeability. The P-wave velocity increased along with the increasing soils strength and time of curing. Higher velocities were recorded for soil stabilised by binder with higher ratio of slag, while lower velocities were obtained for higher ratio of cement, respectively. The effectiveness of P-waves for measuring soil strength is explained by its physical nature, as it passes along the fastest path in the structure of the soil, which is directly related to the strength and stiffness of specimen.

Overall, the experiments proved the direct effects of the proportions of binders on the permeability, compactness and strength of the stabilised soil. For comparison we used the experiments on three different rations of binders added to soil samples. The highest permeability of soil was recorded by samples with increased amount of cement, while the lowest permeability was recorded by increased proportions of slag. Thus, the stabilised soil with higher binder ratio shown higher strength and increased velocity of P-waves compared to the samples with the higher water content. Our results can be considered in similar studies on dredged silts using admixture of the stabilising agents in various ratios to increase soil strength. Future

research can also include the experiments on changing binder ratio and developing more criteria for the S/S treatment of silts.

Acknowledgements

References

[1] J.-M. Bian and B.-T. Wang. Study on shear strength of unsaturated soils based on the saturated soils. In *2011 International Conference on Electric Technology and Civil Engineering (ICETCE)*, pages 2656–2659, 2011. doi: 10.1109/ICETCE.2011.5775686.

[2] J. Jin. Research of soil compactness tested by instant vibration method. In *2011 International Conference on Electric Technology and Civil Engineering (ICETCE)*, pages 585–588, 2011. doi: 10.1109/ICETCE.2011.5774579.

[3] J. Wu, G. Yang, X. Wang, and W. Li. PZT-based soil compactness measuring sheet using electromechanical impedance. *IEEE Sensors Journal*, 20(17):10240–10250, 2020. doi: 10.1109/JSEN.2020.2991580.

[4] X. Wang, X. Dong, Z. Zhang, J. Zhang, G. Ma, and X. Yang. Compaction quality evaluation of subgrade based on soil characteristics assessment using machine learning. *Transportation Geotechnics*, 32:100703, 2022. doi: 10.1016/j.trgeo.2021.100703.

[5] Z. Gao and J. Chai. Method for predicting unsaturated permeability using basic soil properties. *Transportation Geotechnics*, 34:100754, 2022. doi: 10.1016/j.trgeo.2022.100754.

[6] C.E. Choong, K T. Wong, S.B. Jang, J.-Y. Song, S.-G. An, C.-W. Kang, Y. Yoon, and M. Jang. Soil permeability enhancement using pneumatic fracturing coupled by vacuum extraction for in-situ remediation: Pilot-scale tests with an artificial neural network model. *Journal of Environmental Chemical Engineering*, 10(1):107075, 2022. doi: 10.1016/j.jece.2021.107075.

[7] L. Pohl, A. Kölbl, D. Uteau, S. Peth, W. Häusler, L. Mosley, P. Marschner, R. Fitzpatrick, and I. Kögel-Knabner. Porosity and organic matter distribution in jarositic phyto tubules of sulfuric soils assessed by combined µCT and NanoSIMS analysis. *Geoderma*, 399:115124, 2021. doi: 10.1016/j.geoderma.2021.115124.

[8] W. Zhang, R. Bai, X. Xu, and W. Liu. An evaluation of soil thermal conductivity models based on the porosity and degree of saturation and a proposal of a new improved model. *International Communications in Heat and Mass Transfer*, 129:105738, 2021. doi: 10.1016/j.icheatmasstransfer.2021.105738.

[9] F.R.A. Ziegler-Rivera, B. Prado, A. Gastelum-Strozzi, J. Márquez, L. Mora, A. Robles, and B. González. Computed tomography assessment of soil and sediment porosity modifications from exposure to an acid copper sulfate solution. *Journal of South American Earth Sciences*, 108:103194, 2021. doi: 10.1016/j.jsames.2021.103194.

[10] B.C. Ball. Pore characteristics of soils from two cultivation experiments as shown by gas diffusivities and permeabilities and air-filled porosities. *European Journal of Soil Science*, 32(4):483–498, 1981. doi: 10.1111/j.1365-2389.1981.tb01724.x.

[11] S. Deviren Saygin, F. Arı, Ç. Temiz, Ş. Arslan, M.A. Ünal, and G. Erpul. Analysis of soil cohesion by fluidized bed methodology using integrable differential pressure sensors for a wide range of soil textures. *Computers and Electronics in Agriculture*, 191:106525, 2021. doi: 10.1016/j.compag.2021.106525.

[12] Y. Kim, A. Satyanaga, H. Rahardjo, H. Park, and A.W.L. Sham. Estimation of effective cohesion using artificial neural networks based on index soil properties: A Singapore case. *Engineering Geology*, 289:106163, 2021. doi: 10.1016/j.enggeo.2021.106163.

[13] V. Marzulli, C.S. Sandeep, K. Senetakis, F. Cafaro, and T. Pöschel. Scale and water effects on the friction angles of two granular soils with different roughness. *Powder Technology*, 377:813–826, 2021. doi: 10.1016/j.powtec.2020.09.060.

[14] J. Zou, G. Chen, and Z. Qian. Tunnel face stability in cohesion-frictional soils considering the soil arching effect by improved failure models. *Computers and Geotechnics*, 106:1–17, 2019. doi: 10.1016/j.compgeo.2018.10.014.

[15] A. Kaya. Relating equal smectite content and basal spacing to the residual friction angle of soils. *Engineering Geology*, 108(3):252–258, 2009. doi: 10.1016/j.enggeo.2009.06.013.

[16] Y. Wang and O.V. Akeju. Quantifying the cross-correlation between effective cohesion and friction angle of soil from limited site-specific data. *Soils and Foundations*, 56(6):1055–1070, 2016. doi: 10.1016/j.sandf.2016.11.009.

[17] E. Stockton, B.A. Leshchinsky, M.J. Olsen, and T.M. Evans. Influence of both anisotropic friction and cohesion on the formation of tension cracks and stability of slopes. *Engineering Geology*, 249:31–44, 2019. doi: 10.1016/j.enggeo.2018.12.016.

[18] J. Ye. 3D liquefaction criteria for seabed considering the cohesion and friction of soil. *Applied Ocean Research*, 37:111–119, 2012. doi: 10.1016/j.apor.2012.04.004.

[19] M. Ohno and K. Fukai. Pavement construction work of a road surface by soil cement concrete that used construction remainder soil. In *Proceedings First International Symposium on Environmentally Conscious Design and Inverse Manufacturing*, pages 638–641, 1999. doi: 10.1109/ECODIM.1999.747690.

[20] J. Ling, Y. Yang, Z. Ma, and G. Yang. Engineering properties and treatment of hydraulically reclaimed saline soil in coastal area. In *2014 Sixth International Conference on Measuring Technology and Mechatronics Automation*, pages 275–278, 2014. doi: 10.1109/ICMTMA.2014.69.

[21] P.P. Kulkarni and J.N. Mandal. Strength evaluation of soil stabilized with nano silica- cement mixes as road construction material. *Construction and Building Materials*, 314:125363, 2022. doi: 10.1016/j.conbuildmat.2021.125363.

[22] T. Zhang, S. Liu, H. Zhan, C. Ma, and G. Cai. Durability of silty soil stabilized with recycled lignin for sustainable engineering materials. *Journal of Cleaner Production*, 248:119293, 2020. doi: 10.1016/j.jclepro.2019.119293.

[23] R.W. Day. *Soil Testing Manual: Procedures, Classification Data, and Sampling Practices*. McGraw Hill Inc., New York, U.S., 2001.

[24] T. Davis. *Geotechnical Testing, Observation, and Documentation*. American Society of Civil Engineers, Reston, Virginia, U.S., 2 edition, 2008.

[25] D. Hillel. *Fundamentals of Soil Physics*. Academic Press, New York, U.S., 1 edition, 1980.

[26] L.A.P. Barbosa, K.M. Gerke, and H.H. Gerke. Modelling of soil mechanical stability and hydraulic permeability of the interface between coated biopore and matrix pore regions. *Geoderma*, 410:115673, 2022. doi: 10.1016/j.geoderma.2021.115673.

[27] I.I. Obianyo, E.N. Anosike-Francis, G.O. Ihekweme, Y. Geng, R. Jin, A.P. Onwualu, and A.B. O. Soboyejo. Multivariate regression models for predicting the compressive strength of bone ash stabilized lateritic soil for sustainable building. *Construction and Building Materials*, 263:120677, 2020. doi: 10.1016/j.conbuildmat.2020.120677.

[28] L. Bakaiyang, J. Madjadoumbaye, Y. Boussafir, F. Szymkiewicz, and M. Duc. Re-use in road construction of a Karal-type clay-rich soil from North Cameroon after a lime/cement mixed treatment using two different limes. *Case Studies in Construction Materials*, 15:e00626, 2021. doi: 10.1016/j.cscm.2021.e00626.

[29] Z. Han, S.K. Vanapalli, J-P. Ren, and W-L. Zou. Characterizing cyclic and static moduli and strength of compacted pavement subgrade soils considering moisture variation. *Soils and Foundations*, 58(5):1187–1199, 2018. doi: 10.1016/j.sandf.2018.06.003.

[30] I. Kamal and Y. Bas. Materials and technologies in road pavements - an overview. *Materials Today: Proceedings; 3rd International Conference on Materials Engineering & Science*, 42:2660–2667, 2021. doi: 10.1016/j.matpr.2020.12.643.

[31] R. Jauberthie, F. Rendell, D. Rangeard, and L. Molez. Stabilisation of estuarine silt with lime and/or cement. *Applied Clay Science*, 50(3):395–400, 2010. doi: 10.1016/j.clay.2010.09.004.

[32] P. Lindh and P. Lemenkova. Resonant frequency ultrasonic P-waves for evaluating uniaxial compressive strength of the stabilized slag–cement sediments. *Nordic Concrete Research*, 65:39–62, 2021. doi: 10.2478/ncr-2021-0012.

[33] M. Arabi and S. Wild. Property changes induced in clay soils when using lime stabilization. *Municipal Engineer*, 6:85–99, 1989.

[34] P. Lindh. *Compaction- and strength properties of stabilised and unstabilised fine-grained tills*. PhD thesis, Lund University, Lund, Sweden, 2004.

[35] C. Liu and R.D. Starcher. Effects of curing conditions on unconfined compressive strength of cement- and cement-fiber-improved soft soils. *Journal of Materials in Civil Engineering*, 25(8):1134–1141, 2013. doi: 10.1061/(ASCE)MT.1943-5533.0000575.

[36] P.J. Venda Oliveira, A.A.S. Correia, and M.R. Garcia. Effect of organic matter content and curing conditions on the creep behavior of an artificially stabilized soil. *Journal of Materials in Civil Engineering*, 24(7):868–875, 2012. doi: 10.1061/(ASCE)MT.1943-5533.0000454.

[37] H. Ghasemzadeh, A. Mehrpajouh, M. Pishvaei, and M. Mirzababaei. Effects of curing method and glass transition temperature on the unconfined compressive strength of acrylic liquid polymer-stabilized kaolinite. *Journal of Materials in Civil Engineering*, 32(8):04020212, 2020. doi: 10.1061/(ASCE)MT.1943-5533.0003287.

[38] A. Aldaood, M. Bouasker, and M. Al-Mukhtar. Effect of the temperature and curing time on the water transfer of lime stabilized gypseous soil. In *Poromechanics V: Proceedings of the Fifth Biot Conference on Poromechanics*, pages 2325–2333, 2013. doi: 10.1061/9780784412992.272.

[39] H. Yu, J. Yin, A. Soleimanbeigi, and W.J. Likos. Effects of curing time and fly ash content on properties of stabilized dredged material. *Journal of Materials in Civil Engineering*, 29(10):04017199, 2017. doi: 10.1061/(ASCE)MT.1943-5533.0002032.

[40] W.-S. Oh and Ta-H. Kim. Dependence of the material properties of lightweight cemented soil on the curing temperature. *Journal of Materials in Civil Engineering*, 26(7):06014008, 2014. doi: 10.1061/(ASCE)MT.1943-5533.0000940.

[41] I.L. Howard and B.K. Anderson. Time-dependent properties of very high moisture content fine grained soils stabilized with portland and slag cement. In *Geotechnical Frontiers 2017*, pages 891–899, 2017. doi: 10.1061/9780784480472.095.

[42] N.C. Consoli, R.C. Cruz, and M.F. Floss. Variables controlling strength of artificially cemented sand: Influence of curing time. *Journal of Materials in Civil Engineering*, 23(5):692–696, 2011. doi: 10.1061/(ASCE)MT.1943-5533.0000205.

[43] A.T.M.Z. Rabbi and J. Kuwano. Effect of curing time and confining pressure on the mechanical properties of cement-treated sand. In *GeoCongress 2012: State of the Art and Practice in Geotechnical Engineering*, pages 996–1005, 2012. doi: 10.1061/9780784412121.103.

[44] S. Chaiyaput, N. Arwaedo, N. Kingnoi, T. Nghia-Nguyen, and J. Ayawanna. Effect of curing conditions on the strength of soil cement. *Case Studies in Construction Materials*, 16:e01082, 2022. doi: 10.1016/j.cscm.2022.e01082.

[45] P. Lindh and P. Lemenkova. Geochemical tests to study the effects of cement ratio on potassium and TBT leaching and the pH of the marine sediments from the Kattegat Strait, Port of Gothenburg, Sweden. *Baltica*, 35(1):47–59, 2022. doi: 10.5200/baltica.2022.1.4.

[46] A.A. Amadi and A.S. Osu. Effect of curing time on strength development in black cotton soil – quarry fines composite stabilized with cement kiln dust (CKD). *Journal of King Saud University - Engineering Sciences*, 30(4):305–312, 2018. doi: 10.1016/j.jksues.2016.04.001.

[47] D. Wang, R. Zentar, and N.E. Abriak. Temperature-accelerated strength development in stabilized marine soils as road construction materials. *Journal of Materials in Civil Engineering*, 29(5):04016281, 2017. doi: 10.1061/(ASCE)MT.1943-5533.0001778.

[48] B. Rekik, M. Boutouil, and A. Pantet. Geotechnical properties of cement treated sediment: influence of the organic matter and cement contents. *International Journal of Geotechnical Engineering*, 3(2):205–214, 2009. doi: 10.3328/IJGE.2009.03.02.205-214.

[49] E.O. Tastan, T.B. Edil, C.H. Benson, and A.H. Aydilek. Stabilization of organic soils with fly ash. *Journal of Geotechnical and Geoenvironmental Engineering*, 137(9):819–833, 2011. doi: 10.1061/(ASCE)GT.1943-5606.0000502.

[50] H. Hasan, H. Khabbaz, and B. Fatahi. Impact of quicklime and fly ash on the geotechnical properties of expansive clay. In *Geo-China 2016: Advances in Pavement Engineering and Ground Improvement*, pages 93–100, 2016. doi: 10.1061/9780784480014.012.

[51] P. Solanki, N. Khoury, and M. Zaman. Engineering behavior and microstructure of soil stabilized with cement kiln dust. In *Geo-Denver 2007: Soil Improvement*, pages 1–10, 2007. doi: 10.1061/40916(235)6.

[52] P. Lindh and P. Lemenkova. Evaluation of different binder combinations of cement, slag and CKD for s/s treatment of TBT contaminated sediments. *Acta Mechanica et Automatica*, 15(4):236–248, 2021. doi: 10.2478/ama-2021-0030.

[53] A. Arulrajah, A. Mohammadinia, A. D'Amico, and S. Horpibulsuk. Effect of lime kiln dust as an alternative binder in the stabilization of construction and demolition materials. *Construction and Building Materials*, 152:999–1007, 2017. doi: 10.1016/j.conbuildmat.2017.07.070.

[54] X. Bian, L. Zeng, X. Li, X. Shi, S. Zhou, and F. Li. Fabric changes induced by super-absorbent polymer on cement–lime stabilized excavated clayey soil. *Journal of Rock Mechanics and Geotechnical Engineering*, 13(5):1124–1135, 2021. doi: 10.1016/j.jrmge.2021.03.006.

[55] S. Andavan and V.K. Pagadala. A study on soil stabilization by addition of fly ash and lime. *Materials Today: Proceedings; International Conference on Materials Engineering and Characterization 2019*, 22:1125–1129, 2020. doi: 10.1016/j.matpr.2019.11.323.

[56] P. Indiramma, Ch. Sudharani, and S. Needhidasan. Utilization of fly ash and lime to stabilize the expansive soil and to sustain pollution free environment – an experimental study. *Materials Today: Proceedings; International Conference on Materials Engineering and Characterization 2019*, 22:694–700, 2020. doi: 10.1016/j.matpr.2019.09.147.

[57] C.A. Mozejko and F.M. Francisca. Enhanced mechanical behavior of compacted clayey silts stabilized by reusing steel slag. *Construction and Building Materials*, 239:117901, 2020. doi: 10.1016/j.conbuildmat.2019.117901.

[58] M.P. Durante Ingunza, K.L. de Araújo Pereira, and O F. dos Santos Junior. Use of sludge ash as a stabilizing additive in soil-cement mixtures for use in road pavements. *Journal of Materials in Civil Engineering*, 27(7):06014027, 2015. doi: 10.1061/(ASCE)MT.1943-5533.0001168.

[59] M.M. Al-Sharif and M.F. Attom. The use of burned sludge as a new soil stabilizing agent. In *National Conference Environmental and Pipeline Engineering 2000*, pages 378–388, 2000. doi: 10.1061/40507(282)42.

[60] P. Lindh. Optimizing binder blends for shallow stabilisation of fine-grained soils. *Proceedings of the Institution of Civil Engineers - Ground Improvement*, 5(1):23–34, 2001. doi: 10.1680/grim.2001.5.1.23.

[61] A. Ahmed. Compressive strength and microstructure of soft clay soil stabilized with recycled bassanite. *Applied Clay Science*, 104:27–35, 2015. doi: 10.1016/j.clay.2014.11.031.

[62] P. Lindh and M.G. Winter. Sample preparation effects on the compaction properties of Swedish fine-grained tills. *Quarterly Journal of Engineering Geology and Hydrogeology*, 36(4):321–330, 2003. doi: 10.1144/1470-9236/03-018.

[63] P. Xu, Q. Zhang, H. Qian, M. Li, and F. Yang. An investigation into the relationship between saturated permeability and microstructure of remolded loess: A case study from Chinese Loess Plateau. *Geoderma*, 382:114774, 2021. doi: 10.1016/j.geoderma.2020.114774.

[64] A. Anagnostopoulos, G. Koukis, N. Sabatakakis, and G. Tsiambaos. Empirical correlations of soil parameters based on Cone Penetration Tests (CPT) for Greek soils. *Geotechnical and Geological Engineering*, 21:377–387, 2003. doi: 10.1023/B:GEGE.0000006064.47819.1a.

[65] H. Källén, A. Heyden, K. Åström, and P. Lindh. Measuring and evaluating bitumen coverage of stones using two different digital image analysis methods. *Measurement*, 84:56–67, 2016. doi: 10.1016/j.measurement.2016.02.007.

[66] V. Lemenkov and P. Lemenkova. Measuring equivalent cohesion C_{eq} of the frozen soils by compression strength using kriolab equipment. *Civil and Environmental Engineering Reports*, 31(2):63–84, 2021. doi: 10.2478/ceer-2021-0020.

[67] X. Huang, R. Horn, and T. Ren. Soil structure effects on deformation, pore water pressure, and consequences for air permeability during compaction and subsequent shearing. *Geoderma*, 406:115452, 2022. doi: 10.1016/j.geoderma.2021.115452.

[68] W. Kongkitkul, T. Saisawang, P. Thitithavoranan, P. Kaewluan, and T. Posribink. Correlations between the surface stiffness evaluated by light-weight deflectometer and degree of compaction. In *Geo-Shanghai 2014: Tunneling and Underground Construction*, pages 65–75, 2014. doi: 10.1061/9780784413449.007.

[69] K. Lee, M. Prezzi, and N. Kim. Subgrade design parameters from samples prepared with different compaction methods. *Journal of Transportation Engineering*, 133(2):82–89, 2007. doi: 10.1061/(ASCE)0733-947X(2007)133:2(82).

[70] M. Bryk. Resolving compactness index of pores and solid phase elements in sandy and silt loamy soils. *Geoderma*, 318:109–122, 2018. doi: 10.1016/j.geoderma.2017.12.030.

[71] W. l. Zou, Z. Han, S.K. Vanapalli, J.-F. Zhang, and G.-T. Zhao. Predicting volumetric behavior of compacted clays during compression. *Applied Clay Science*, 156:116–125, 2018. doi: 10.1016/j.clay.2018.01.036.

[72] S.J. Wasman, M.C. McVay, K. Beriswill, D. Bloomquist, J. Shoucair, and D. Horhota. Study of laboratory compaction system variance using an Automatic Proctor Calibration Device. *Journal of Materials in Civil Engineering*, 25(4):429–437, 2013. doi: 10.1061/(ASCE)MT.1943-5533.0000599.

[73] L. Di Matteo, F. Bigotti, and R. Ricco. Best-fit models to estimate modified Proctor properties of compacted soil. *Journal of Geotechnical and Geoenvironmental Engineering*, 135(7):992–996, 2009. doi: 10.1061/(ASCE)GT.1943-5606.0000022.

[74] O. Boudlal and B. Melbouci. Study of the behavior of aggregates demolition by the Proctor and CBR tests. In *GeoHunan International Conference 2009: Material Design, Construction, Maintenance, and Testing of Pavements*, pages 75–80, 2009. doi: 10.1061/41045(352)12.

[75] L. Barden and G.R. Sides. Engineering behavior and structure of compacted clay. *Journal of the Soil Mechanics and Foundations Division*, 96(4):1171–1200, 1970. doi: 10.1061/JSFEAQ.0001434.

[76] M. Jibon and D. Mishra. Light weight deflectometer testing in Proctor molds to establish resilient modulus properties of fine-grained soils. *Journal of Materials in Civil Engineering*, 33(2):06020025, 2021. doi: 10.1061/(ASCE)MT.1943-5533.0003582.

[77] A. Aragón, M.G. García, R.R. Filgueira, and Ya.A. Pachepsky. Maximum compactibility of Argentine soils from the Proctor test: The relationship with organic carbon and water content. *Soil and Tillage Research*, 56(3):197–204, 2000. doi: 10.1016/S0167-1987(00)00144-6.

[78] H. Bayat, S. Asghari, M. Rastgou, and G.R. Sheykhzadeh. Estimating Proctor parameters in agricultural soils in the Ardabil plain of Iran using support vector machines, artificial neural networks and regression methods. *CATENA*, 189:104467, 2020. doi: 10.1016/j.catena.2020.104467.

[79] A.B.J.C. Nhantumbo and A.H. Cambule. Bulk density by Proctor test as a function of texture for agricultural soils in Maputo province of Mozambique. *Soil and Tillage Research*, 87(2):231–239, 2006. doi: 10.1016/j.still.2005.04.001.

[80] A. Alaoui, J. Lipiec, and H.H. Gerke. A review of the changes in the soil pore system due to soil deformation: A hydrodynamic perspective. *Soil and Tillage Research*, 115-116:1–15, 2011. doi: 10.1016/j.still.2011.06.002.

[81] ASTM Standard D698. *Standard Test Methods for Laboratory Compaction Characteristics of Soil Using Standard Effort*. ASTM International, West Conshohocken, PA, U. S., ICS Code: 93.020 edition, 2007. doi: 10.1520/D0698-07E01.

[82] ASTM Standard D1557. *Standard Test Methods for Laboratory Compaction Characteristics of Soil Using Modified Effort*. ASTM International, West Conshohocken, PA, U. S., 2009. doi: 10.1520/D1557-09.

[83] L. Wang, X. Xie, and H. Luan. Influence of laboratory compaction methods on shear performance of graded crushed stone. *Journal of Materials in Civil Engineering*, 23(10):1483–1487, 2011. doi: 10.1061/(ASCE)MT.1943-5533.0000323.

[84] A. Alaoui and A. Helbling. Evaluation of soil compaction using hydrodynamic water content variation: Comparison between compacted and non-compacted soil. *Geoderma*, 134(1):97–108, 2006. doi: 10.1016/j.geoderma.2005.08.016.

[85] M. Livneh and N.A. Livneh. Use of the one-point Proctor modified compaction method in family compaction curves possessing a limited trend characteristic. In *Airfield and Highway Pavement 2013: Sustainable and Efficient Pavements*, pages 1304–1315, 2013. doi: 10.1061/9780784413005.110.

[86] A.F. Elhakim. Estimation of soil permeability. *Alexandria Engineering Journal*, 55(3):2631–2638, 2016. doi: 10.1016/j.aej.2016.07.034.

[87] Y. Yu, J.A. Huisman, A. Klotzsche, H. Vereecken, and L. Weihermüller. Coupled full-waveform inversion of horizontal borehole ground penetrating radar data to estimate soil hydraulic parameters: A synthetic study. *Journal of Hydrology*, 610:127817, 2022. doi: 10.1016/j.jhydrol.2022.127817.

[88] J. Zhou, S. Laumann, and T.J. Heimovaara. Applying aluminum-organic matter precipitates to reduce soil permeability in-situ: A field and modeling study. *Science of The Total Environment*, 662:99–109, 2019. doi: 10.1016/j.scitotenv.2019.01.109.

[89] A. Takai, T. Inui, and T. Katsumi. Evaluating the hydraulic barrier performance of soil-bentonite cutoff walls using the piezocone penetration test. *Soils and Foundations*, 56(2):277–290, 2016. doi: 10.1016/j.sandf.2016.02.010.

[90] Y.X. Lim, S.A. Tan, and K.-K. Phoon. Interpretation of horizontal permeability from piezocone dissipation tests in soft clays. *Computers and Geotechnics*, 107:189–200, 2019. doi: 10.1016/j.compgeo.2018.12.001.

[91] Y. Liu, S.J. Chen, K. Sagoe-Crentsil, and W. Duan. Predicting the permeability of consolidated silty clay via digital soil reconstruction. *Computers and Geotechnics*, 140:104468, 2021. doi: 10.1016/j.compgeo.2021.104468.

[92] T. Shibi and Y. Ohtsuka. Influence of applying overburden stress during curing on the unconfined compressive strength of cement-stabilized clay. *Soils and Foundations*, 61(4):1123–1131, 2021. doi: 10.1016/j.sandf.2021.03.007.

[93] N. Kardani, A. Zhou, S.-L. Shen, and M. Nazem. Estimating unconfined compressive strength of unsaturated cemented soils using alternative evolutionary approaches. *Transportation Geotechnics*, 29:100591, 2021. doi: 10.1016/j.trgeo.2021.100591.

[94] F. Mousavi, E. Abdi, S. Ghalandarayeshi, and D.S. Page-Dumroese. Modeling unconfined compressive strength of fine-grained soils: Application of pocket penetrometer for predicting soil strength. *CATENA*, 196:104890, 2021. doi: 10.1016/j.catena.2020.104890.

[95] A. Ahmed. Compressive strength and microstructure of soft clay soil stabilized with recycled bassanite. *Applied Clay Science*, 104:27–35, 2015. doi: https://doi.org/10.1016/j.clay.2014.11.031.

[96] J.B. Burland. On the compressibility and shear strength of natural clays. *Géotechnique*, 40(3):329–378, 1990. doi: 10.1680/geot.1990.40.3.329.

[97] S.M. Rao and P. Shivananda. Compressibility behaviour of lime-stabilized clay. *Geotechnical and Geological Engineering*, 23:301–311, 2005. doi: 10.1007/s10706-004-1608-2.

[98] M. Al-Mukhtar, S. Khattab, and J.-F. Alcover. Microstructure and geotechnical properties of lime-treated expansive clayey soil. *Engineering Geology*, 139-140:17–27, 2012. doi: 10.1016/j.enggeo.2012.04.004.

[99] A. al-Swaidani, I. Hammoud, and A. Meziab. Effect of adding natural pozzolana on geotechnical properties of lime-stabilized clayey soil. *Journal of Rock Mechanics and Geotechnical Engineering*, 8(5):714–725, 2016. doi: 10.1016/j.jrmge.2016.04.002.

[100] C. Phetchuay, S. Horpibulsuk, A. Arulrajah, C. Suksiripattanapong, and A. Udomchai. Strength development in soft marine clay stabilized by fly ash and calcium carbide residue based geopolymer. *Applied Clay Science*, 127-128:134–142, 2016. doi: 10.1016/j.clay.2016.04.005.

[101] V. Lemenkov and P. Lemenkova. Testing deformation and compressive strength of the frozen fine-grained soils with changed porosity and density. *Journal of Applied Engineering Sciences*, 11(2):113–120, 2021. doi: 10.2478/jaes-2021-0015.

[102] V. Lemenkov and P. Lemenkova. Using TeX markup language for 3D and 2D geological plotting. *Foundations of Computing and Decision Sciences*, 46(3):43–69, 2021. doi: 10.2478/fcds-2021-0004.

[103] P.K. Robertson, S. Sasitharan, J.C. Cunning, and D.C. Sego. Shear-wave velocity to evaluate in-situ state of Ottawa sand. *Journal of Geotechnical Engineering*, 121(3):262–273, 1995. doi: 10.1061/(ASCE)0733-9410(1995)121:3(262).

[104] K. Komal, S. Bawa, and S. KantSharma. Laboratory investigation on the effect of polypropylene and nylon fiber on silt stabilized clay. *Materials Today: Proceedings; International Conference on Smart and Sustainable Developments in Materials, Manufacturing and Energy Engineering*, 52:1368–1376, 2021. doi: 10.1016/j.matpr.2021.11.123.

[105] H. Källén, A. Heyden, and P. Lindh. Estimation of grain size in asphalt samples using digital image analysis. In *Proceedings: Applications of Digital Image Processing XXXVII*, volume 9217, pages 292–300, 2014. doi: 10.1117/12.2061730.

[106] Swedish Institute for Standards. SIS: Geotechnical investigation and testing – Laboratory testing of soil – Part 7: Unconfined compression test (ISO 17892-7:2017), 2017. ISO 17892-7:2017.

[107] Swedish Institute for Standards. SIS: Earthworks – Part 4: Soil treatment with lime and/or hydraulic binders. online, 2018. SS-EN 16907-4:2018.

[108] Swedish Institute for Standards. Geotechnical investigation and testing - Laboratory testing of soil - Part 11: Permeability tests (ISO 17892-11:2019). online, 2019. Article no: STD-80010356.

[109] BSI Standards Publication. Cement part 1: Composition, specifications and conformity criteria for common cements. European Standard (English version), 2011. BS EN 197-1:2011. ISBN: 978 0 580 68241 4.

[110] Thomas Concrete Group. Teknisk Information. Slagg Bremen Mald granulerad masugnsslagg för användning i betong och bruk enligt SS 137003. https://thomasconcretegroup.com/us/, 2014. Retrieved 2014-01-16 from Thomas Concrete Group.

[111] N. Ryden, U. Dahlen, P. Lindh, and A. Jakobsson. Impact non-linear reverberation spectroscopy applied to non-destructive testing of building materials. *The Journal of the Acoustical Society of America*, 140(4):3327–3327, 2016. doi: 10.1121/1.4970601.